

AD-A260 828

MENTATION PAGE

Form Approved
OMB No. 0704-0188

(2)



estimated to average 1 hour per response, including the time for reviewing instructions, searching existing data sources, and reviewing the collection of information. Send comments regarding this burden estimate or any other aspect of this burden to Washington Headquarters Services, Directorate for Information Operations and Reports, 1215 Jefferson Avenue, S.W., Washington, D.C. 20540, and to the Office of Management and Budget, Paperwork Reduction Project (0704-0188), Washington, D.C. 20503.

REPORT DATE
17/18/93

3. REPORT TYPE AND DATES COVERED

Technical

4. TITLE AND SUBTITLE

Thermomechanical response of shape memory composites

5. FUNDING NUMBERS

DAAL03-92-G-0123

6. AUTHOR(S)

James G. Boyd and Dimitris C. Lagoudas

7. PERFORMING ORGANIZATION NAME(S) AND ADDRESS(ES)

Rensselaer Polytechnic Institute
Dept. of Civil & Env. Engineering, JEC 4049
110 - 8th Street
Troy, NY 12180-3590

DTIC

S ELEC REFORC ORGANIZATION
FEB 19 1993 REPORT NUMBER
C D

9. SPONSORING/MONITORING AGENCY NAME(S) AND ADDRESS(ES)

U. S. Army Research Office
P. O. Box 12211
Research Triangle Park, NC 27709-2211

10. SPONSORING/MONITORING AGENCY REPORT NUMBER

ARO 30378-4EG-URI

11. SUPPLEMENTARY NOTES

The view, opinions and/or findings contained in this report are those of the author(s) and should not be construed as an official Department of the Army position, policy, or decision, unless so designated by other documentation.

12a. DISTRIBUTION/AVAILABILITY STATEMENT

Approved for public release; distribution unlimited.

12b. DISTRIBUTION CODE

13. ABSTRACT (Maximum 200 words)

The Mori-Tanaka micromechanics method is used to predict the effective properties of composite materials consisting of a polymer matrix reinforced by a fiber made of a transformation shape memory effect (SME) material. The composite response is plotted for combinations of the following scenarios: (1) isothermal longitudinal and transverse stress input, (2) stress-free thermal loading, (3) constant fiber thermoelastic properties, and (4) thermoelastic fiber properties that vary with the martensite volume fraction. For the case of an isothermal stress input, the composite transformation stress, the maximum transformation strain, and the hysteresis are all reduced vis-a-vis the monolithic SME material. In contrast to a monolithic SME material, stress-free thermal loading of a SME composite can produce a transformation strain. It is shown that closed form solutions for the effective martensite and austenite start temperatures can be derived, that they are sensitive to the stress-free reference temperature of the fiber, and that the stress-free austenite and martensite start temperatures are higher than those of the monolithic SME material.

14. SUBJECT TERMS

93-03269



18pg

15. NUMBER OF PAGES

17

16. PRICE CODE

17. SECURITY CLASSIFICATION OF REPORT

UNCLASSIFIED

OF THIS PAGE

UNCLASSIFIED

18. SECURITY CLASSIFICATION OF ABSTRACT

UNCLASSIFIED

20. LIMITATION OF ABSTRACT

UL

DTIC QUALITY INSPECTED 3

Thermomechanical response of shape memory composites

James G. Boyd

Dimitris C. Lagoudas

Center for Mechanics of Composites
 Texas A&M University
 College Station, TX 77843-3141

ABSTRACT

The Mori-Tanaka micromechanics method is used to predict the effective properties of composite materials consisting of a polymer matrix reinforced by a fiber made of a transformation shape memory effect (SME) material. The composite response is plotted for combinations of the following scenarios: (1) isothermal longitudinal and transverse stress input, (2) stress-free thermal loading, (3) constant fiber thermoelastic properties, and (4) thermoelastic fiber properties that vary with the martensite volume fraction. For the case of an isothermal stress input, the composite transformation stress, the maximum transformation strain, and the hysteresis are all reduced vis-a-vis the monolithic SME material. In contrast to a monolithic SME material, stress-free thermal loading of a SME composite can produce a transformation strain. It is shown that closed form solutions for the effective martensite and austenite start temperatures can be derived, that they are sensitive to the stress-free reference temperature of the fiber, and that the stress-free austenite and martensite start temperatures are higher than those of the monolithic SME material.

1. INTRODUCTION

Active shape memory effect (SME) materials allow for the fabrication of structures with intrinsic control of shape and vibration parameters such as stiffness, natural frequency, and damping. The SME is usually due to either the stress induced transformation between austenite and martensite or the reorientation of martensite variants. For both the transformation and the reorientation SME, an active composite can be made by surrounding a prestressed martensitic SME fiber with a non-SME matrix material. When the composite is heated, usually by passing an electric current through the SME fiber, the martensite is transformed into austenite and the fiber contracts, thereby producing the activation. Upon cooling, the austenite transforms into martensite, and the internal stresses (sometimes called eigenstresses) within the matrix return the composite structure to its original shape.

Constitutive equations describing the thermomechanical behavior of SME composites are needed to enable their efficient production and service. In phenomenological constitutive modelling, the form of the equations and the constants in the equations are determined from experiments. Phenomenological modelling is descriptive, but not explanatory. Micromechanical constitutive modelling consists of solving a small-scale boundary value problem and then averaging the solution to obtain the effective (or overall) composite properties. Because micromechanics is explanatory, it allows for the systematic design of composite materials.

Accession For	
NTIS CRA&I	<input checked="" type="checkbox"/>
DTIC TAB	<input type="checkbox"/>
Unannounced	<input type="checkbox"/>
Justification	
By	
Distribution /	
Availability Codes	
Dist	Avail and/or Special
A-1	23

In the present paper, the Mori-Tanaka² micromechanics method is used to predict the thermomechanical response of composites consisting of transformation SME fibers and non-SME matrices. The matrix of such a composite must be capable of accommodating the large strains associated with the SME of the fiber. Polymers are therefore currently envisaged as matrix materials. Although the large fiber transformation strains will cause viscoelasticity in the polymer matrix, the matrix is herein assumed to be linear thermoelastic. In part 2, the one-dimensional transformation SME constitutive equations of Tanaka are extended to three dimensions. In part 3, the Mori-Tanaka micromechanics method is presented. The thermomechanical behavior of both the SME fiber and the composite are discussed in part 4.

Throughout the paper, superscripts denote qualitative description of the associated variables, whereas subscripts denote tensorial components.

2. SME FIBER CONSTITUTIVE EQUATIONS

Liang and Rogers³ have extended Tanaka's⁴ one-dimensional transformation SME equations to three dimensions. The present derivation is similar to the method of Liang and Rogers in that it assumes that the transformation is unaffected by the hydrostatic stress. However, the present derivation of the tangent mechanical and thermal stiffness tensors differs from the derivation of Liang and Rogers. The stress-strain equation of state is given by

$$\sigma_{ij} = C_{ijkl} \epsilon_{kl}^e = C_{ijkl} (\epsilon_{kl} - \epsilon_{kl}^t - \alpha_{kl} \Delta T) \quad (1)$$

where C_{ijkl} , α_{ij} , ϵ_{ij}^e , ϵ_{ij} , ϵ_{ij}^t , and ΔT are the elastic stiffness tensor, the thermoelastic expansion tensor, the elastic strain, the total infinitesimal strain, the transformation strain, and $\Delta T = T - T^0$, where T^0 is the stress-free reference temperature. The elastic stiffness and thermoelastic expansion tensors are approximated here by the rule of mixtures

$$C_{ijkl} = C_{ijkl}^A + \xi (C_{ijkl}^M - C_{ijkl}^A), \quad \alpha_{kl} = \alpha_{kl}^A + \xi (\alpha_{kl}^M - \alpha_{kl}^A), \quad (2)$$

where the superscripts A and M stand for austenite and martensite, and ξ , an internal variable representing the volume fraction of martensite, is given by

$$\xi = 1 - \exp[a^M (M^{0s} - T) + b^M \sigma] \quad M^s \leq T \leq M^s \quad (3)$$

during the martensitic transformation and

$$\xi = \exp[a^A (A^{0s} - T) + b^A \sigma] \quad A^s \leq T \leq A^s \quad (4)$$

during the reverse transformation. M^{0s} and A^{0s} represent the stress-free martensite and austenite start temperatures, respectively. The stress dependence of the transformation temperatures is given by

$$\begin{aligned} M^s &= M^{0s} + \frac{1}{C^M} \sigma, & M^f &= M^{0f} + \frac{1}{C^M} \sigma, \\ A^s &= A^{0s} + \frac{1}{C^A} \sigma, & A^f &= A^{0f} + \frac{1}{C^A} \sigma, \end{aligned} \quad (5)$$

where C^M and C^A are the martensitic and austenitic stress influence coefficients. Assuming that the transformation is complete when $\xi = 0.99$, the constants a^M , b^M , a^A , and b^A are given by

$$\begin{aligned} a^M &= \frac{\ln(0.01)}{(M^s - M^f)}, & b^M &= \frac{a^M}{C^M}, \\ a^A &= \frac{\ln(0.01)}{(A^s - A^f)}, & b^A &= \frac{a^A}{C^A}. \end{aligned} \quad (6)$$

By assuming that the stress-induced SME is isotropic, these three-dimensional equations for ξ were obtained from the one-dimensional equations by replacing the one-dimensional stress by the effective stress, $\bar{\sigma}$, where $\bar{\sigma} = (\frac{3}{2}\sigma'_{ij}\sigma'_{ij})^{\frac{1}{2}}$, and the deviatoric stress σ'_{ij} is given by $\sigma'_{ij} = \sigma_{ij} - \frac{1}{3}\sigma_{kk}\delta_{ij}$. The rate of transformation can be obtained by applying the chain rule to (3) and (4) to yield

$$\dot{\xi} = \frac{\partial \xi}{\partial T} \dot{T} + \frac{\partial \xi}{\partial \bar{\sigma}} \dot{\bar{\sigma}} \quad (7)$$

The transformation strain is due solely to that part of ξ that is stress-induced. In other words, it is assumed that a stress-free thermal loading of the SME material produces no transformation strain because all of the martensite variants form with equal probability and the transformation is volume conserving, or isochoric. An applied stress, however, favors the growth of those martensitic variants which are oriented to yield the largest transformation strains.

By assuming that the elastic response is also isotropic, the three-dimensional transformation strain rate can be obtained from the one-dimensional equation as follows:

$$\dot{\epsilon}^t = -\frac{\Omega}{D} \frac{\partial \xi}{\partial \bar{\sigma}} \dot{\bar{\sigma}} \rightarrow \dot{\epsilon}^t_{ij} = -\frac{3\Omega}{2D} \frac{\partial \xi}{\partial \bar{\sigma}} \dot{\sigma}'_{ij} = H \dot{\sigma}'_{ij}, \quad (8)$$

where the transformation tensor, Ω , can be obtained from the maximum isothermal transformation strain (which corresponds to $\xi = 1$) and the one-dimensional elastic modulus, D , using $\epsilon^{tmax} = -\frac{\Omega}{D}$. During the martensitic and reverse transformations, respectively, the "hardness" parameter, H , is

$$H = \begin{cases} \frac{3\Omega}{2D} b^M (1 - \xi) & M^f \leq T \leq M^s \\ -\frac{3\Omega}{2D} b^A \xi & A^s \leq T \leq A^f \end{cases} \quad (9)$$

$H = 0$ during transformation-free deformation.

Equations (1) through (9) complete the constitutive description of the SME material. However, the tangent mechanical and thermal stiffness tensors are needed in the Mori-Tanaka micromechanics method. The tangent mechanical and thermal stiffnesses L_{ijkl} and l_{ij} , respectively, are defined by

$$\dot{\sigma}_{ij} = L_{ijkl} \dot{\epsilon}_{kl} + l_{ij} \dot{T}. \quad (10)$$

In order to derive these tangent stiffness tensors, equation (1) is written in rate form as

$$\begin{aligned} \dot{\sigma}_{ij} &= C_{ijkl} \dot{\epsilon}^e_{kl} + \dot{C}_{ijkl} \epsilon^e_{kl} \\ &= C_{ijkl} (\dot{\epsilon}_{kl} - \dot{\epsilon}^t_{kl} - \alpha_{kl} \dot{T} - \dot{\alpha}_{kl} \Delta T) + \dot{C}_{ijkl} \epsilon^e_{kl}. \end{aligned} \quad (11)$$

Equations (2) and (7) thru (9) can be substituted into (11) to yield

$$\begin{aligned} \dot{\sigma}_{ij} = & C_{ijkl} \dot{\epsilon}_{kl} - H C_{ijkl} (\dot{\sigma}_{kl} - \frac{1}{3} \dot{\sigma}_{rr} \delta_{kl}) - C_{ijkl} \alpha_{kl} \dot{T} \\ & - C_{ijkl} (\alpha_{kl}^M - \alpha_{kl}^A) \Delta T \left(\frac{\partial \xi}{\partial T} \dot{T} + \frac{\partial \xi}{\partial \bar{\sigma}} \dot{\bar{\sigma}} \right) + (C_{ijkl}^M - C_{ijkl}^A) \epsilon_{kl}^e \left(\frac{\partial \xi}{\partial T} \dot{T} + \frac{\partial \xi}{\partial \bar{\sigma}} \dot{\bar{\sigma}} \right). \end{aligned} \quad (12)$$

By introducing the term

$$\Phi_{ijmn} = I_{ijmn} + H C_{ijmn} \quad (13)$$

and collecting the terms multiplying \dot{T} and $\dot{\bar{\sigma}}$, equation (12) can be rewritten as

$$\begin{aligned} \dot{\sigma}_{mn} \Phi_{ijmn} = & C_{ijkl} \dot{\epsilon}_{kl} + H C_{ijkl} \frac{1}{3} \dot{\sigma}_{rr} \delta_{kl} \\ & + \left[(C_{ijkl}^M - C_{ijkl}^A) \epsilon_{kl}^e - C_{ijkl} (\alpha_{kl}^M - \alpha_{kl}^A) \Delta T \right] \frac{\partial \xi}{\partial \bar{\sigma}} \dot{\bar{\sigma}} \\ & + \left\{ \left[(C_{ijkl}^M - C_{ijkl}^A) \epsilon_{kl}^e - C_{ijkl} (\alpha_{kl}^M - \alpha_{kl}^A) \Delta T \right] \frac{\partial \xi}{\partial T} - C_{ijkl} \alpha_{kl} \right\} \dot{T}. \end{aligned} \quad (14)$$

The temperature rate \dot{T} is assumed to be a known input. Recall that both $\dot{\sigma}_{ij}$ and $\dot{\epsilon}_{ij}$ are known from the non-tangent form of the constitutive equations, equations (1) thru (9). Therefore, all of the terms in equation (14) are known, and the tangent response can be determined. For example, during an isothermal transformation the tangent stiffness is given by

$$L_{mnkl} = \frac{C_{ijkl}}{\Phi_{ijmn}} + \frac{1}{\Phi_{ijmn} \dot{\epsilon}_{kl}} \left\{ H C_{ijop} \frac{1}{3} \dot{\sigma}_{rr} \delta_{op} + \left[(C_{ijop}^M - C_{ijop}^A) \epsilon_{op}^e - C_{ijop} (\alpha_{op}^M - \alpha_{op}^A) \Delta T \right] \frac{\partial \xi}{\partial \bar{\sigma}} \dot{\bar{\sigma}} \right\}. \quad (15)$$

During transformation-free thermomechanical loading, the tangent response is given by

$$\dot{\sigma}_{ij} = C_{ijkl} \dot{\epsilon}_{kl} - C_{ijkl} \alpha_{kl} \dot{T}, \quad (16)$$

so that $L_{ijkl} = C_{ijkl}$ and $l_{ij} = -C_{ijkl} \alpha_{kl}$.

3. MICROMECHANICS

3.1 General expressions for the effective composite properties

Equations (17) thru (32). Hill's⁵ "direct approach" to effective composite properties, are general relationships that are independent of the micromechanics method used to obtain the concentration tensors. The thermomechanical constitutive relations of the phases $v = m$ (matrix) and $v = f$ (fiber) are given by

$$\dot{\sigma}_{ij}^v = L_{ijkl}^v \dot{\epsilon}_{kl}^v + l_{ij}^v \dot{T}, \quad v = m, f \quad (17)$$

and

$$\dot{\epsilon}_{ij}^v = M_{ijkl}^v \dot{\sigma}_{kl}^v + m_{ij}^v \dot{T}, \quad v = m, f \quad (18)$$

where L_{ijkl}^v and M_{ijkl}^v are the tangent stiffness and compliance tensors, respectively. The thermal strain tensor m_{ij}^v and the thermal stress tensor l_{ij}^v are related by

$$l_{ij}^v = -L_{ijkl}^v m_{kl}^v. \quad (19)$$

Similarly, the composite response is given by the effective constitutive equations

$$\dot{\sigma}_{ij}^c = L_{ijkl}^c \dot{\epsilon}_{kl}^c + l_{ij}^c \dot{T} \quad (20)$$

and

$$\dot{\epsilon}_{ij}^c = M_{ijkl}^c \dot{\sigma}_{kl}^c + m_{ij}^c \dot{T} \quad (21)$$

with

$$l_{ij}^c = -L_{ijkl}^c m_{kl}^c. \quad (22)$$

The composite stress and strain rates are given by the volume averages

$$\dot{\sigma}_{ij}^c = c^m \dot{\sigma}_{ij}^m + c^f \dot{\sigma}_{ij}^f \quad (23)$$

and

$$\dot{\epsilon}_{ij}^c = c^m \dot{\epsilon}_{ij}^m + c^f \dot{\epsilon}_{ij}^f, \quad (24)$$

where c^v denotes the volume fraction of the v^{th} phase. The local constituent stress and strain fields, assumed to be uniform within each phase, are given in terms of the composite fields by

$$\dot{\sigma}_{ij}^v = B_{ijkl}^v \dot{\sigma}_{kl}^c + b_{ij}^v \dot{T}, \quad v = m, f \quad (25)$$

and

$$\dot{\epsilon}_{ij}^v = A_{ijkl}^v \dot{\epsilon}_{kl}^c + a_{ij}^v \dot{T}, \quad v = m, f, \quad (26)$$

where B_{ijkl}^v , A_{ijkl}^v , b_{ij}^v and a_{ij}^v are the stress, strain, thermal stress and thermal strain concentration tensors, respectively. The concentration tensors are constrained by the relations

$$c^m B_{ijkl}^m + c^f B_{ijkl}^f = I_{ijkl}, \quad (27)$$

$$c^m A_{ijkl}^m + c^f A_{ijkl}^f = I_{ijkl}, \quad (28)$$

$$c^m b_{ij}^m + c^f b_{ij}^f = 0, \quad (29)$$

and

$$c^m a_{ij}^m + c^f a_{ij}^f = 0, \quad (30)$$

where I_{ijkl} is the fourth order identity tensor. The effective composite tangent stiffness and compliance tensors, respectively, are

$$L_{ijkl}^c = c^m L_{ijmn}^m A_{mnkl}^m + c^f L_{ijmn}^f A_{mnkl}^f \quad (31)$$

and

$$M_{ijkl}^c = c^m M_{ijmn}^m B_{mnkl}^m + c^f M_{ijmn}^f B_{mnkl}^f. \quad (32)$$

Note that the effective stiffness is not the volume average of the constituent stiffnesses.

The thermal stress and strain concentration tensors can be determined using the decomposition scheme of Benveniste and Dvorak.⁶ The decomposition allows for the determination of the thermal concentration tensors as a function of the mechanical concentration tensors and the constituent thermomechanical properties. The thermal stress and strain concentration tensors are given as

$$b_{ij}^v = (I_{ijkl} - B_{ijkl}^v) (M_{klmn}^m - M_{klmn}^f)^{-1} (m_{mn}^f - m_{mn}^m), \quad v = m, f, \quad (33)$$

and

$$a_{ij}^v = (I_{ijkl} - A_{ijkl}^v) (L_{klmn}^m - L_{klmn}^f)^{-1} (l_{mn}^f - l_{mn}^m), \quad v = m, f. \quad (34)$$

The effective composite thermal properties are given by

$$l_{ij}^c = l_{ij}^m + c^f (L_{ijkl}^f - L_{ijkl}^m) A_{klmn}^f (L_{mnop}^f - L_{mnop}^m)^{-1} (l_{op}^f - l_{op}^m), \quad (35)$$

and

$$m_{ij}^c = m_{ij}^m + c^f (M_{ijkl}^f - M_{ijkl}^m) B_{klmn}^f (M_{mnop}^f - M_{mnop}^m)^{-1} (m_{op}^f - m_{op}^m). \quad (36)$$

Note that equations (33) thru (36) are general relationships that are independent of the micromechanics method used to obtain the mechanical concentration tensors. This decomposition method requires that the effects of thermal and mechanical loads can be obtained separately. This linearity requirement is violated during the SME phase transformation. In the current incremental formulation, it is assumed that the SME equations are piecewise linear, that is, linear within each increment. The accumulated error will be small if small increments are used.

3.2 The Mori-Tanaka micromechanics method

From inspection of equations (17) thru (36), it is apparent that the effective composite thermomechanical constitutive equations may be obtained from the evaluation of the mechanical concentration tensors. The mechanical concentration tensors are herein determined using the Benveniste reinterpretation of the Mori-Tanaka method.

Eshelby's method,^{7,8} sometimes called the "equivalent inclusion method", is a means of predicting the effective properties of dilutely reinforced composite materials. The term "dilute" means that the reinforcement phase is of a sufficiently small volume fraction that the units of reinforcement, such as particles, whiskers or fibers, do not interact. The Mori-Tanaka method is an approximate extension of Eshelby's method to the case of non-dilute volume fractions. The Mori-Tanaka method is a "mean field" theory, meaning that the model assumes that the stress and the strain are uniform within each phase of the composite. The model makes use of the reinforcement volume fraction and the reinforcement shape, but the size of the units of reinforcement play no part in the method. It is assumed that the temperature is uniform throughout the composite. For isothermal conditions, the concentration tensors are given by the Mori-Tanaka micromechanics method as

$$B_{ijkl}^v = W_{ijmn}^v (c^m I_{mnkl} + c^f W_{mnkl}^f)^{-1}, \quad v = m, f, \quad (37)$$

and

$$A_{ijkl}^v = T_{ijmn}^v (c^m I_{mnkl} + c^f T_{mnkl}^f)^{-1}, \quad v = m, f. \quad (38)$$

The dilute strain concentration tensor T_{ijkl}^f and the dilute stress concentration tensor W_{ijkl}^f are defined as

$$T_{ijkl}^f = \left[I_{ijkl} + S_{ijmn} (L_{mnop}^m)^{-1} (L_{opkl}^f - L_{opkl}^m) \right]^{-1}, \quad (39)$$

and

$$W_{ijkl}^f = L_{ijmn}^f T_{mnop}^f M_{opkl}^m, \quad (40)$$

with

$$T_{ijkl}^m = W_{ijkl}^m = I_{ijkl}. \quad (41)$$

The solution of the mechanical problem requires the evaluation of the Eshelby tensor, S_{ijkl} , which is a function of the reinforcement shape and the matrix stiffness. The Eshelby tensor relates the unconstrained transformation strains and thermal strains, called "eigenstrains" in the vocabulary of Mura,⁸ to the actual transformation strains and thermal strains in the composite. Within the composite, these eigenstrains are partially constrained due to the mismatch of phase mechanical and thermal stiffnesses. Because the matrix stiffness is herein assumed to be constant, the Eshelby tensor must be calculated only once, even though the SME fiber stiffness varies. If the matrix stiffness varies, as it does during plastic deformation of metal matrix composites, then it is necessary to calculate the Eshelby tensor in each load step.⁹ For the case of an ellipsoidal reinforcement in a generally anisotropic matrix, the Eshelby tensor must be evaluated numerically. For the case of isotropic matrix materials, closed form solutions for the Eshelby tensor have been determined for a number of ellipsoidal reinforcement shapes. For the present case of circular cylindrical fibers aligned in the x_3 direction in an isotropic matrix, the components of the Eshelby tensor are given by

$$\begin{aligned} S_{1111} = S_{2222} &= \frac{1}{4(1-\nu)} \left(\frac{5}{2} - 2\nu \right), \quad S_{3333} = 0, \quad S_{1122} = S_{2211} = \frac{1}{4(1-\nu)} \left(-\frac{1}{2} + 2\nu \right), \\ S_{3311} &= 0, \quad S_{1133} = \frac{\nu}{2(1-\nu)}, \quad S_{1212} = \frac{1}{4(1-\nu)} \left(\frac{3}{2} - 2\nu \right), \quad S_{2323} = S_{1313} = \frac{1}{4}, \end{aligned} \quad (42)$$

where ν is the matrix Poisson ratio. Note that the Eshelby tensor, and therefore the concentration tensors, are not symmetric for the case of cylindrical fibers in an isotropic matrix.

4. RESULTS AND DISCUSSION

4.1 The effective transformation temperatures

The composite will start and finish the phase transformation when the fiber starts and finishes its transformation. In other words, $M^{cs} = M^s$, $M^{cf} = M^f$, $A^{cs} = A^s$ and $A^{cf} = A^f$, where the superscript "c" denotes "composite" and M^s , M^f , A^s and A^f are given by (5). In order to obtain equations for the effective, or composite, transformation temperatures, it is necessary to relate the fiber stress in (5) to the composite stress and the temperature. Unfortunately, the fiber

stress and the composite stress and temperature are in general related by the rate equation (25), which includes path dependent concentration tensors. However, under special conditions, such as non-transformational (thermoelastic) deformation, (25) may be integrated in closed form to yield a relation between the fiber stress and the composite stress and temperature. M^{cs} and A^{cs} can be derived in closed form because they are reached via a non-transformational (thermoelastic) deformation. Consider the case of initial loading of an austenitic ($\xi = 0$) composite. Prior to the start of the martensite transformation, (25) may be written as

$$\sigma_{ij}^v = B_{ijkl}^{vea} \sigma_{kl}^e + b_{ij}^{vea} \Delta T, \quad v = m, f \quad (43)$$

where the superscript "ea" denotes the elastic concentration tensor corresponding to an austenitic fiber. The effective stress-free martensite start temperature, M^{cos} , can be determined in closed form by substituting (43) into (5), with $\sigma_{ij}^e = 0$, to yield

$$M^{cos} = M^{os} + \frac{1}{C^M} \sigma^f = M^{os} + \frac{\bar{b}^{fea}}{C^M} (\Delta T \Delta T)^{\frac{1}{2}}, \quad (44)$$

where the superscript "f" denotes "fiber", not "finish", $\bar{b}^{fea} = (\frac{1}{2} b_{ij}^{fea} b_{ij}^{fea})^{\frac{1}{2}}$, and $b_{ij}^{fea} = b_{ij}^{ea} - \frac{1}{3} b_{rr}^{ea} \delta_{ij}$. By noting that both C^M and \bar{b}^{fea} are positive semi-definite, it is apparent from (44) that the effective threshold M^{cos} is never less than the matrix threshold M^{os} because the thermal eigenstresses raise the fiber M^s temperature. Thus, although the fiber and composite transformation temperatures are equal ($M^{cs} = M^s$), it does NOT follow that the fiber and composite stress-free martensite start temperatures are equal, i.e. $M^{cos} \neq M^{os}$. Equation (44) illustrates the importance of the relative values of M^{os} and T^o and $\frac{1}{C^M} \bar{b}^{fea}$ in determining the temperature increment ΔT that will initiate the stress-free composite martensite transformation. The relationship between M^{cos} , ΔT and T is plotted in Figures 1(a) and 1(b). Note from Figure 1(a) that if $M^{os} > T^o$ and the slope $\frac{1}{C^M} \bar{b}^{fea} \geq 1$, then any ΔT will result in a temperature that is below M^{cos} . From Figure 1(b), it is apparent that if $M^{os} < T^o$ and the slope $\frac{1}{C^M} \bar{b}^{fea} > 1$, then there is a region $\Delta T^o < \Delta T < \Delta T^{**}$ in which T is above the M^{cos} threshold. In this case, the martensitic transformation may be initiated by either cooling or heating the stress-free composite. The effective austenite start temperature can also be determined by following the previous procedure. Consider the case of initial loading of a martensitic ($\xi = 1$) composite. Prior to the start of the austenitic transformation, (25) may be written as

$$\sigma_{ij}^v = B_{ijkl}^{vem} \sigma_{kl}^e + b_{ij}^{vem} \Delta T, \quad v = m, f \quad (45)$$

where the superscript "em" denotes the elastic concentration tensor corresponding to a martensitic fiber. The effective stress-free austenite start temperature, A^{cos} , can be determined in closed form by substituting (45) into (5), with $\sigma_{ij}^e = 0$, to yield

$$A^{cos} = A^{os} + \frac{1}{C^A} \sigma^f = A^{os} + \frac{\bar{b}^{fem}}{C^A} (\Delta T \Delta T)^{\frac{1}{2}}. \quad (46)$$

The relationship between A^{cos} , ΔT and T is plotted in Figures 1(c) and 1(d). Note from Figure 1(c) that if $A^{os} > T^o$ and the slope $\frac{1}{C^A} \bar{b}^{fem} \geq 1$, then no ΔT will result in a temperature that

is above A^{cs} . From Figure 1(d), it is apparent that if $A^{cs} < T^o$ and the slope $\frac{1}{C\lambda} \bar{b}^{fcm} > 1$, then there is a region $\Delta T^{\dagger} < \Delta T < \Delta T^{\ddagger}$ in which the temperature is above the A^{cs} threshold. In this case, the austenitic transformation may be suppressed by either cooling or heating the stress-free composite.

This procedure for determining M^{cs} and A^{cs} is not suitable for determining the effective stress-free finish temperatures M^{cf} and A^{cf} because (25) cannot be integrated in closed form during the transformation leading to M^{cf} and A^{cf} .

T^o will probably depend on the composite manufacturing method. The dependence of M^{cs} and A^{cs} on T^o indicates the importance of modelling the thermomechanics of the composite fabrication.

The stress dependence of M^{cs} and A^{cs} can be determined by substituting (43) into (5) with $\Delta T = 0$ to yield

$$M^{cs} = M^s = M^{os} + \frac{1}{CM} \bar{\sigma}^f = M^{os} + \frac{1}{CM} \left(\frac{3}{2} B_{ijkl}^{fca} B_{ijmn}^{fca} \sigma_{kl}^c \sigma_{mn}^c \right)^{\frac{1}{2}}, \quad (47)$$

where $B_{ijkl}^{fca} = B_{ijkl}^{fca} - \frac{1}{3} B_{rrkl}^{fca} \delta_{ij}$. In a similar manner, the stress dependence of A^{cs} can be obtained as

$$A^{cs} = A^s = A^{os} + \frac{1}{CA} \bar{\sigma}^f = A^{os} + \frac{1}{CA} \left(\frac{3}{2} B_{ijkl}^{fcm} B_{ijmn}^{fcm} \sigma_{kl}^c \sigma_{mn}^c \right)^{\frac{1}{2}}. \quad (48)$$

Both M^{cs} and A^{cs} increase linearly with σ_{ij}^c , but the effect is now anisotropic: different components of σ_{ij}^c have different influences on M^{cs} and A^{cs} . The effective transformation is anisotropic and pressure dependent even though the SME fiber is isotropic and pressure-independent. Also, the effective transformation tensor is no longer a scalar.

This procedure for determining the stress dependence of M^{cs} and A^{cs} is not suitable for determining the stress dependence of M^{cf} and A^{cf} because (25) cannot be integrated in closed form during the transformation leading to M^{cf} and A^{cf} . In monolithic SME materials, the M^f and A^f lines are parallel to the M^s and A^s lines in a stress-temperature space. The present authors are currently studying the history dependent shape of the M^{cf} and A^{cf} lines.

4.2 The SME fiber response

The thermomechanical behavior of a NiTi SME fiber presented in Figures 2 thru 4. The NiTi material properties are given in Table 1. Figure 2 indicates that for temperatures greater than A^f the SME is replaced by pseudoelasticity due to transformation. For Figure 2, it was assumed that the fiber elastic modulus was constant and equal to the average of the austenitic (E^A) and martensitic (E^M) elastic moduli. The effects of a variable elastic modulus may be seen in Figure 3. The results of a stress-free thermal loading are shown in Figure 4. Recall that a stress-free thermal transformation does not produce a transformation strain. Therefore, the total strain in Figure 4 is equal to the thermoelastic strain. Note that in the case of a variable thermoelastic expansion coefficient, the finish strain does not equal the start strain even though the finish temperature is equal to the start temperature.

4.3 The SME composite response

The thermomechanical effects of manufacturing, such as applying a prestress to the SME fiber, are not considered herein. The response of a SME composite ($c^f = 0.30$) is given in Figures 5 thru 7. In Figures 5 and 7, it was assumed that the fiber thermoelastic moduli are constant and equal to the average of E^A and E^M . Figure 5 indicates that the isothermal transformation stress, the isothermal transformation strain, and the isothermal hysteresis are all reduced in the composite vis-a-vis the monolithic SME material. By comparing the longitudinal and transverse responses, it may be seen that the transformation stress and the maximum transformation strain are highly anisotropic, which indicates that the effective stress influence coefficient and transformation tensors are anisotropic. The effects of variable fiber elastic moduli may be seen in Figure 6. The longitudinal composite response is more sensitive than the monolithic SME material response (Figure 3) to the effects of variable elastic moduli. However, the transverse composite response is less sensitive than the monolithic fiber response (Figure 3) to the effects of variable elastic moduli because the compliant matrix dominates the transverse response. Figure 7 indicates that, in contrast to the monolithic SME material (Figure 4), thermal loading of a composite that is free of net stress ($\sigma_{fj}^0 = 0$) results in a transformation strain. During the transformation, which begins at approximately 23°C , the composite thermal expansion coefficient varies because the fiber mechanical tangent stiffness and the mechanical stress concentration tensor vary. The variable composite thermal expansion coefficient is not a result of variable fiber thermoelastic moduli, which were assumed to be constant in Figure 7. After the transformation is complete, the composite thermal expansion coefficient is equal to its value prior to the start of the transformation; this would not be true in the case of variable fiber thermoelastic moduli.

5. SUMMARY

The Mori-Tanaka micromechanics method was used to predict the effective properties of SME composite materials consisting of a polymer matrix reinforced by a transformation SME fiber. For the case of an isothermal stress input, the composite transformation stress, the maximum transformation strain, and the hysteresis were all reduced vis-a-vis the monolithic SME material. In contrast to a monolithic SME material, stress-free thermal loading of a SME composite can produce a transformation strain. It was shown that closed form solutions for the effective martensite and austenite start temperatures can be derived, that they are sensitive to the stress-free reference temperature (T^0) of the fiber, and that the stress free transformation start temperatures are higher than those of the monolithic SME material.

In future research, the present authors will consider: (1) the effects of matrix viscoelasticity, (2) the influence of manufacturing effects such as residual stresses and alteration of T^0 , and (3) the shape and path dependence of the transformation finish temperatures in a stress-temperature hyperspace.

6. ACKNOWLEDGMENTS

The authors gratefully acknowledge the financial support of the Army Research Office University Research Initiative on Interdisciplinary Basic Research in Smart Materials and Structures, Grant No. DAALO3-92-G-0123, monitored by Dr. G.L. Anderson.

7. REFERENCES

1. Y. Benveniste, "A new approach to the application of Mori-Tanaka's theory in composite materials," *Mechanics of Materials*, Vol. 6, No. 3, pp.147-157, 1987.
2. T. Mori and K. Tanaka, "Average stress in matrix and average elastic energy of materials with misfitting inclusion," *Acta Metallurgica*, Vol. 21, pp. 571-574, 1973.
3. C. Liang and C. A. Rogers, "The multi-dimensional constitutive relations of shape memory alloys," *Proceedings of the AIAA 32nd Structures, Structural Dynamics and Materials Conference*, 1991.
4. Y. Sato and K. Tanaka, "Estimation of the energy dissipation in alloys due to stress-induced martensitic transformation," *Res Mechanica*, Vol. 23, pp. 381-393, 1988.
5. R. Hill, "A self-consistent mechanics of composite materials," *Journal of the Mechanics and Physics of Solids*, Vol. 13, pp. 213-222, 1965.
6. Y. Benveniste and G. J. Dvorak, "On a correspondence between mechanical and thermal effects in two phase composites," *Micromechanics and Inhomogeneity*, pp.65-81, Springer-Verlag, NY, 1990.
7. J. D. Eshelby, "The determination of the elastic field of the ellipsoidal inclusion. and related problems," *Proceedings of the Royal Society of London*, Vol. A241, pp. 376-396, 1957.
8. T. Mura, *Micromechanics of Defects in Solids*, Martinus-Nijhoff, 1982.
9. D. C. Lagoudas, A. C. Gavazzi and H. Nigam, "Elastoplastic behavior of metal matrix composites based on incremental plasticity and the Mori-Tanaka average scheme," *Journal of Computational Mechanics*, Vol. 8, pp. 193-203, 1991.
10. A. C. Gavazzi and D. C. Lagoudas, "On the numerical evaluation of Eshelby's tensor and its application to elastoplastic fibrous composites," *Journal of Computational Mechanics*, Vol. 7, pp.13-19, 1991.
11. C. Y. Lei and M. H. Wu, "Thermomechanical properties of NiTi-base shape memory alloys," *Smart Structures and Materials, AD-Vol. 24/AMD-Vol. 123, ASME*, pp.73-77, 1991.

Table 1. Fiber and matrix properties

NiTi material properties

$$E^A = 30.0 \times 10^3 \text{ MPa}$$

$$E^M = 13.0 \times 10^3 \text{ MPa}$$

$$\nu = 0.33$$

$$\alpha^A = 12.5 \times 10^{-6} / ^\circ\text{C}$$

$$\alpha^M = 18.5 \times 10^{-6} / ^\circ\text{C}$$

$$M^s = 23^\circ\text{C}$$

$$M^f = 5^\circ\text{C}$$

$$A^s = 29^\circ\text{C}$$

$$A^f = 51^\circ\text{C}$$

$$C^M = 11.3 \text{ MPa}/^\circ\text{C}$$

$$C^A = 4.5 \text{ MPa}/^\circ\text{C}$$

$$\Omega = 0.91 \times 10^3 \text{ MPa}$$

Polymer material properties

$$E = 2.0 \times 10^3 \text{ MPa}$$

$$\nu = 0.33$$

$$\alpha = 75 \times 10^{-6} / ^\circ\text{C}$$

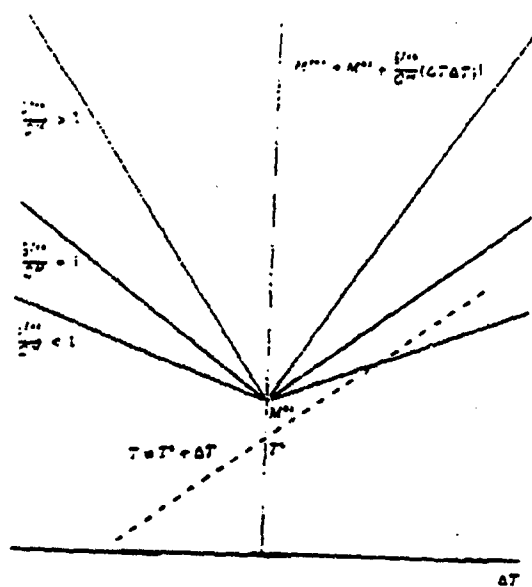
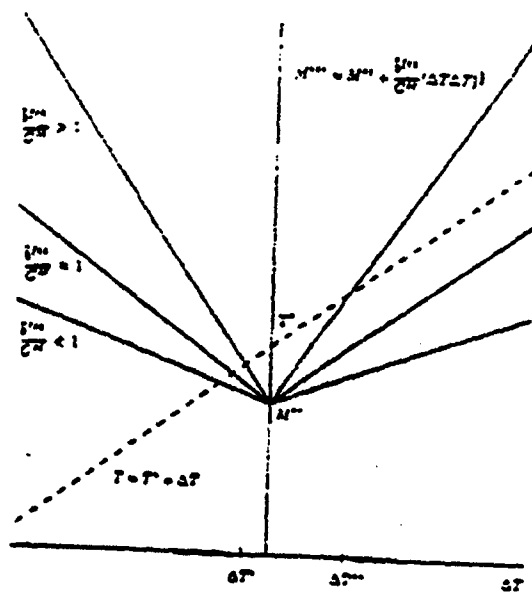
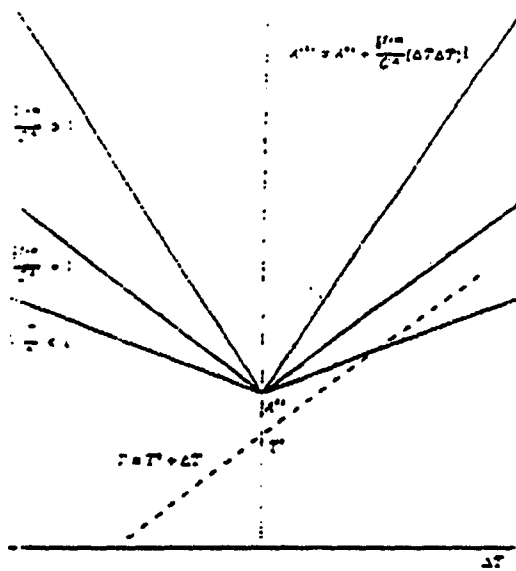
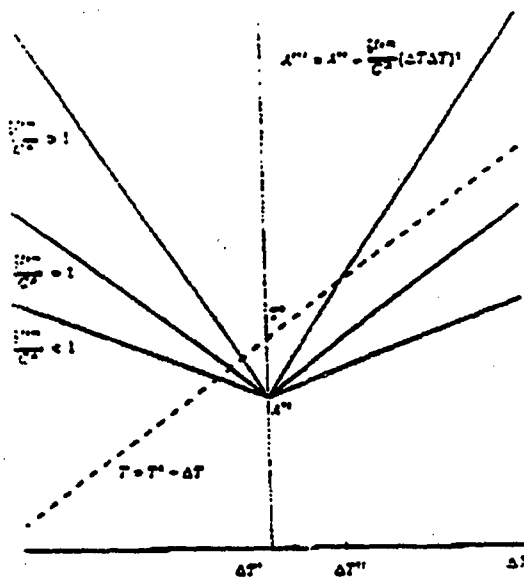
(a) $M^{ss} > T^0$ (b) $M^{ss} < T^0$

Figure 1. The effective stress-free transformation start temperatures M^{ss} and A^{ss} vs ΔT .



(c) $A'' > T''$



(d) $A'' < T''$

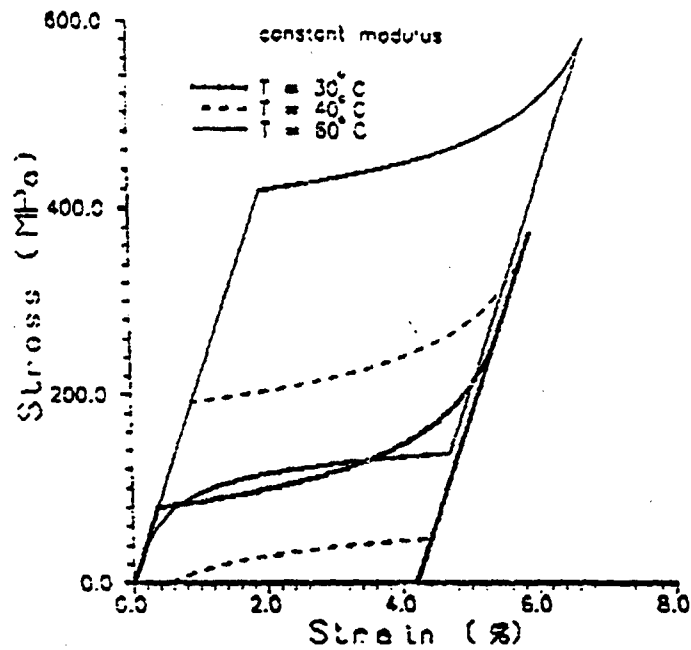


Figure 2. The monolithic ($c^f = 1.0$) SME material response, constant thermoelastic moduli.

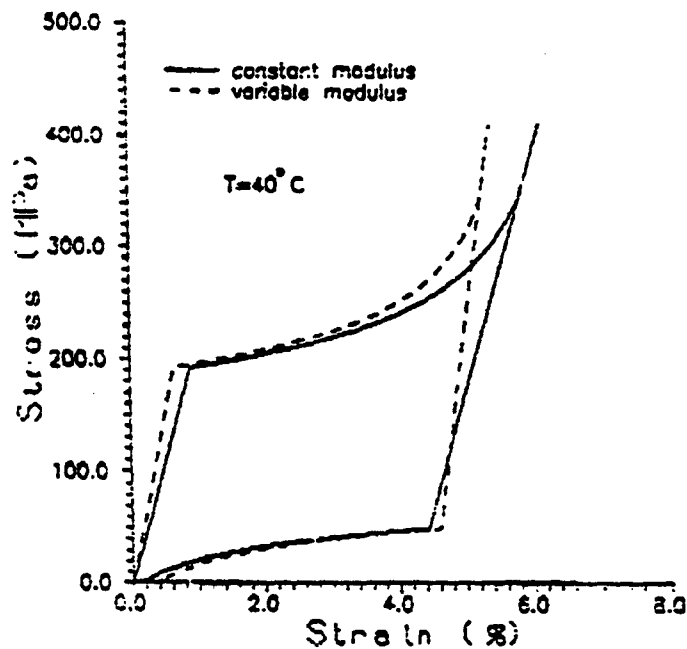


Figure 3. The monolithic ($c^f = 1.0$) SME material response, variable thermoelastic moduli.

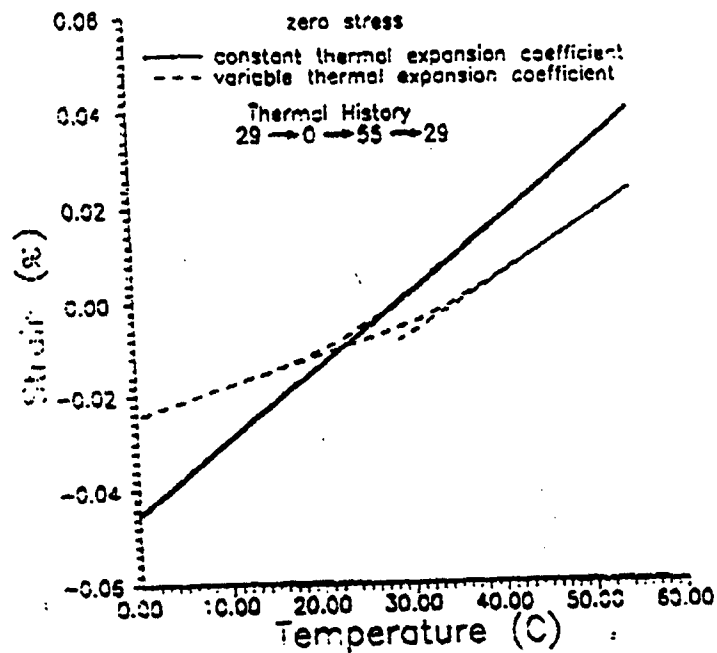


Figure 4. The monolithic ($c^f = 1.0$) SME material response, stress-free thermal loading.

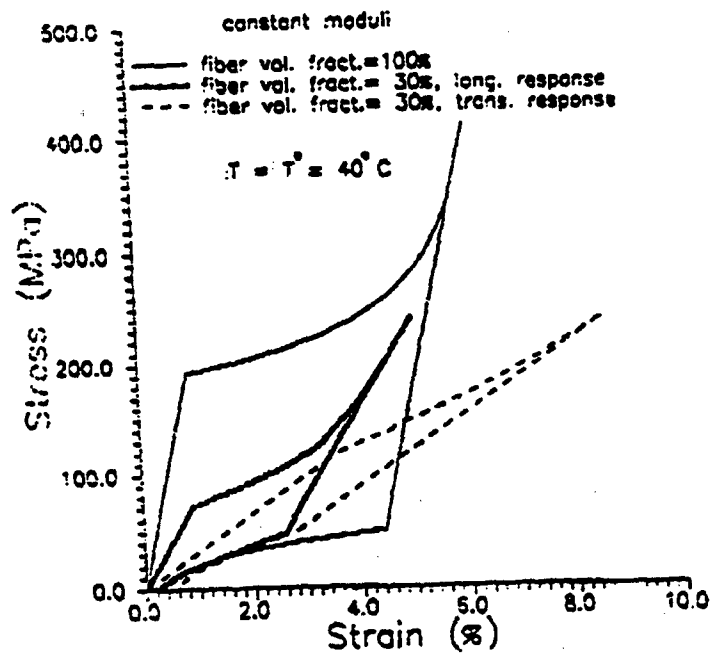


Figure 5. The isothermal SME composite response, constant fiber thermoelastic moduli.

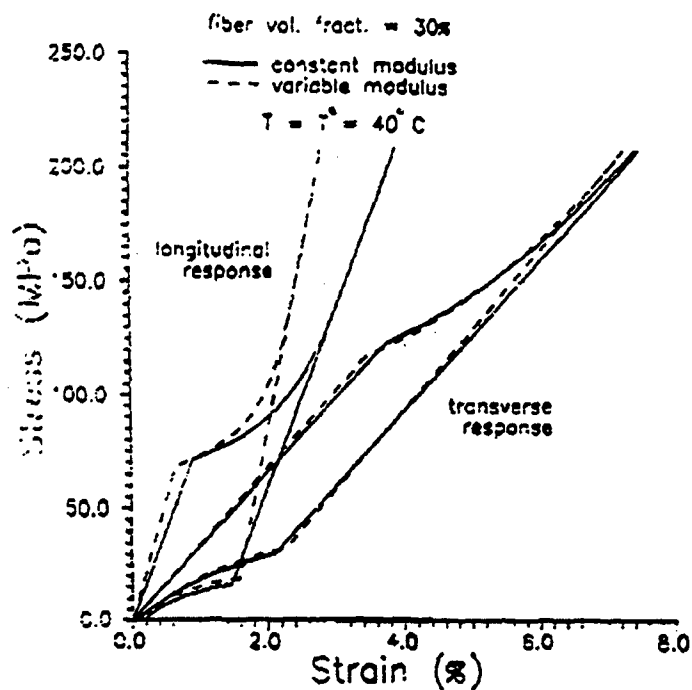


Figure 6. The isothermal SME composite response, variable fiber thermoelastic moduli.

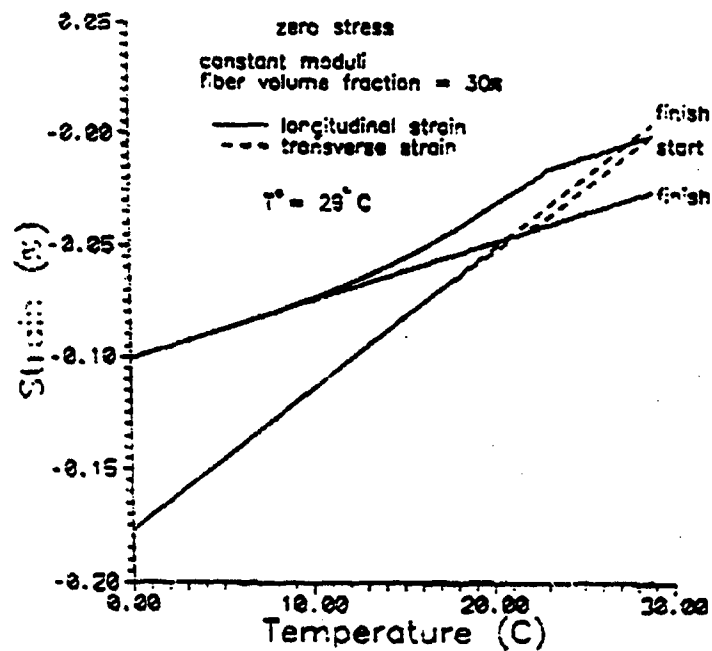


Figure 7. The SME composite response, stress-free thermal loading.

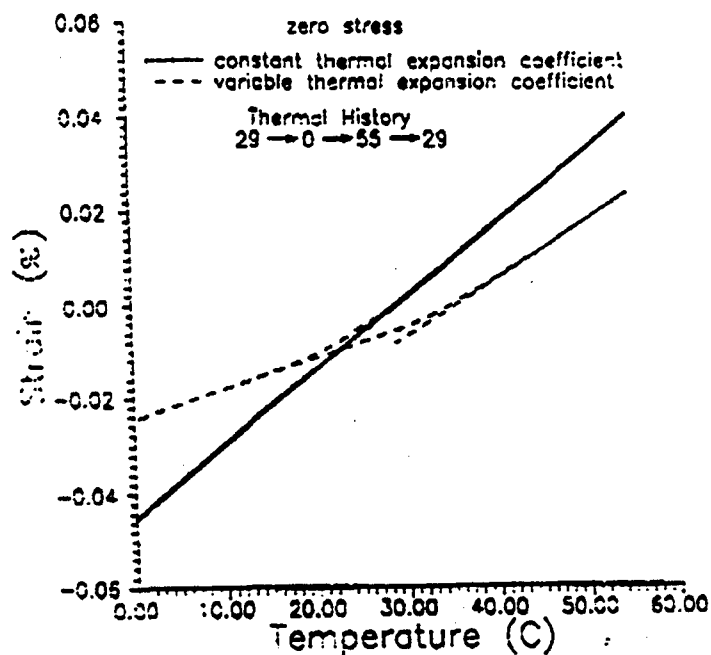


Figure 4. The monolithic ($c' = 1.0$) SME material response, stress-free thermal loading.

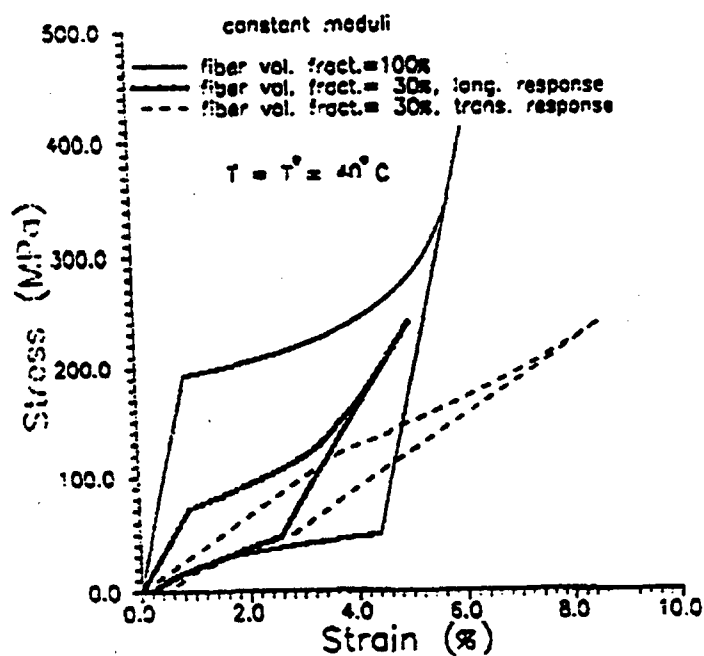


Figure 5. The isothermal SME composite response, constant fiber thermoelastic moduli.

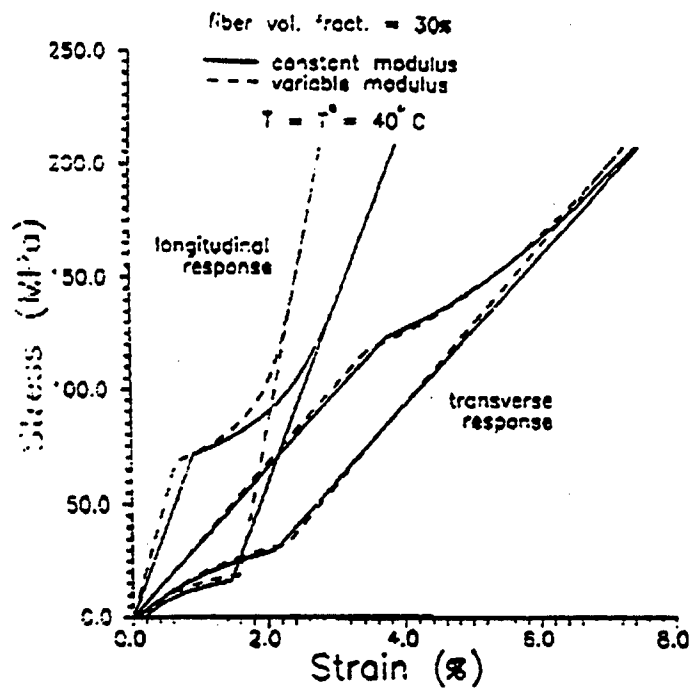


Figure 6. The isothermal SME composite response, variable fiber thermoelastic moduli.

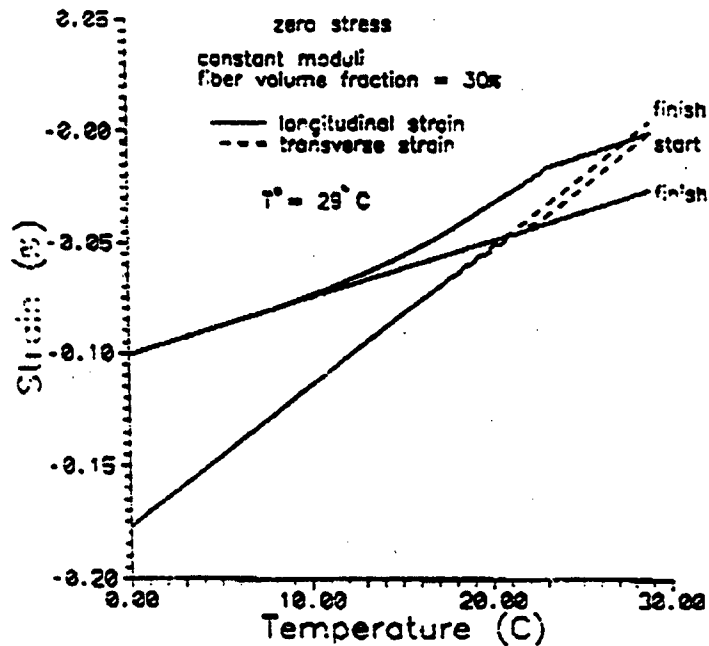


Figure 7. The SME composite response, stress-free thermal loading.